

# THE 4TH INTERNATIONAL CONFERENCE ON ALUMINUM ALLOYS

## FATIGUE CRACK GROWTH IN ALUMINUM-BASE ALLOYS

A. K. Vasudevan<sup>1</sup> and K. Sadananda<sup>2</sup>

1. Office of Naval Research, Code-332, 800 N. Quincy Street, Arlington, VA 22217-5660, USA

2. Naval Research Laboratory, Code-6323, Washington, DC 20375, USA

### Abstract

The fatigue crack growth (FCG) of aluminum-based alloys is characterized using the "new" concepts recently developed by the authors. The concepts are based on the premise that cyclic damage requires "two independent loading parameters" for an unambiguous description. Growth of a fatigue crack is governed by two thresholds; one in terms of each loading parameter that must be satisfied simultaneously for crack growth to occur. The two thresholds are given by the asymptotic limits in a plot of  $\Delta K_{th}$  and  $K_{max}$ , defined as a "fundamental threshold curve." It is observed that the two thresholds depend on the environment and microstructure. Using these concepts, published FCG data on several aluminum-base alloys were examined and their subsequent behavior broadly classified into "five" groups that depended on the relative roles of plasticity and environment.

### Introduction

There is a general perception in the fatigue crack growth (FCG) literature that the near-threshold regions are strongly affected by premature crack closure believed to be originated either from plasticity or from the asperity [1,2]. Recently, we have critically reexamined the crack closure concepts [3-11] and have concluded that (a) there is no crack closure from plasticity [3, 9-11], (b) when asperity-induced closure occur, its contribution is about 1/5th of what is normally estimated from experiments based the changing slopes in a load-displacement curve [9-11], and (c) complete closure is possible only when the crack volume can be completely filled with oxide or corrosion product [3-11]. Thus, in most experimentally observed cases, crack closure is either non-existent (as in plasticity) or small (as in asperity) to provide an overall rationale for the observed reduction in  $\Delta K_{th}$  vs R, and its dependence on microstructure, environment, etc.

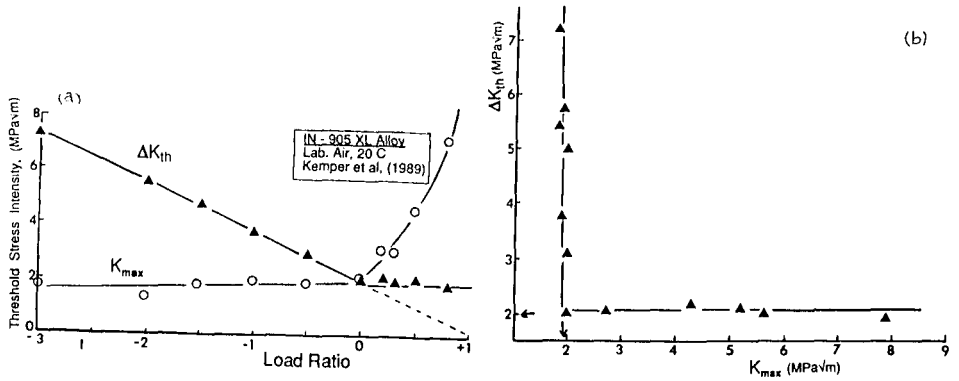


Figure 1. (a) Variation of  $\Delta K_{th}$  and  $K_{max}$  with load ratio  $R$  for a IN-905 Aluminum alloy in lab. air, and (b) a replot of (a) as  $K_{max}$  dependence on  $\Delta K_{th}$ .

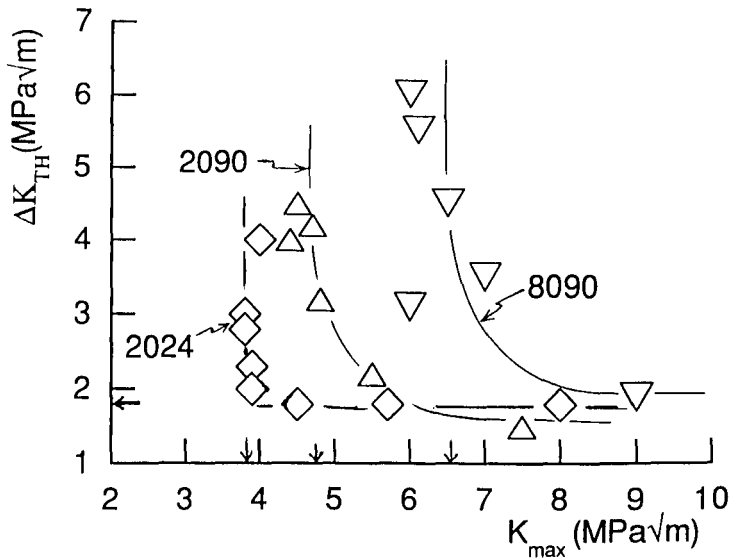


Figure 2.  $\Delta K_{th}^*$  and  $K_{max}^*$  plot comparing the two planar slip deforming Al-Li alloys (8090 & 2090) with a conventional homogeneously deforming 2024-T3 alloy.

As a result, an alternate model is proposed to account for the observed effects that is "intrinsic" to the FCG process. Based on these concepts, the entire FCG behavior is classified into "five" groups that depends on the  $\Delta K_{th}$ - R relation. This article briefly discusses fatigue crack growth behavior and the required driving forces in terms of  $\Delta K$  and  $K_{max}$  using relevant examples from aluminum-base alloys.

### Old and new Concepts in FCG Phenomena

At near-threshold region, FCG behavior is generally given in terms of the variation in threshold stress intensity  $\Delta K_{th}$  with load ratio R. It is observed that most materials show a linear reduction in  $\Delta K_{th}$  with increase in R, in laboratory air. Fig.1a shows such a plot for an al-alloy [12] for R ranging from -3 to +0.8. On the same plot,  $K_{max}$  variation is also shown. The result shows that  $\Delta K_{th}$  decreased with R until  $R \sim 0$  and leveled off at  $R > 0$ . In the early interpretation [1] this decrease  $\Delta K_{th}$  with R in Fig.1a is attributed to premature crack closure up to  $R \sim 0$ , beyond which closure effects are considered as negligible. Under fully reversed loading ( $R < 0$ ), it is associated with closure due to flattening of the asperities from the compressive contact between the two crack surfaces. If  $\Delta K_{th}$  was plotted against  $K_{max}$  (from Figure 1a), one gets a L-shaped curve shown in figure 2b, defining a critical threshold in  $\Delta K_{th}$  (as  $\Delta K_{th}^*$ ) and in  $K_{max}$  (as  $K_{max}^*$ ); shown by the arrows in Fig 1b. These critical parameters define the  $K_{max}$ -controlled region (at  $R < 0$ ) and the  $\Delta K_{th}$ - controlled region (at  $R > 0$ ); in Fig. 1a. The two critical stress intensity parameters are necessary minimum conditions for FCG, independent of any crack closure mechanisms, load history or testing methods. For a given material and loading condition, the  $\Delta K_{th}^*$  and  $K_{max}^*$  can vary with environment and microstructure. The degree and magnitude of the effect depends upon the deformation mode in a material and the aggressiveness of the environment. As an example, the microstructural effect on the  $\Delta K_{th}$ - $K_{max}$  curve is shown in Fig. 2. The comparison is made in Al-Li alloy system with varying degree of planar slip deformation. As the degree of planar slip deformation decreases the  $K_{max}^*$  also decreases toward that of the homogeneously deforming 2024 alloy; while  $\Delta K_{th}^*$  remaining constant. These two critical parameters vary with each other depending on the material and environment.

This variation can be examined from the available threshold data on Al-base alloys and their composites for each environment, namely vacuum and lab air. The data are plotted in Fig. 3 in terms of  $\Delta K_{th}$  versus  $K_{max}$ , governed by the linear relationships:  $\Delta K_{th}^* = K_{max}^* (1-R^*)$ . Most of the vacuum data (monolithic al-alloys) lie on a single line and the laboratory air data on another. There is a subtle variation from the type reinforcements. Salient part of the figure is that the data lies on a single line irrespective of the composition, strength, modulus and fatigue

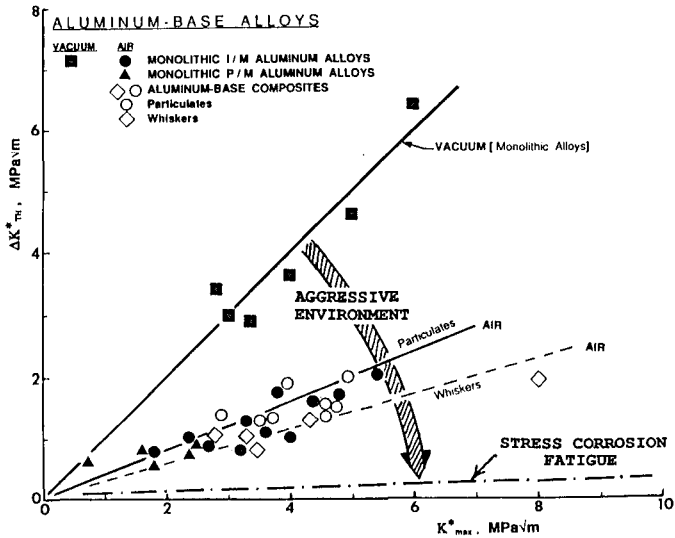


Figure 3. Illustrations of the role of environment affecting the critical stress intensity parameters,  $\Delta K_{th}^*$  and  $K_{max}^*$ , for the aluminum-base composites. For comparison, vacuum data of monolithic alloys is shown.

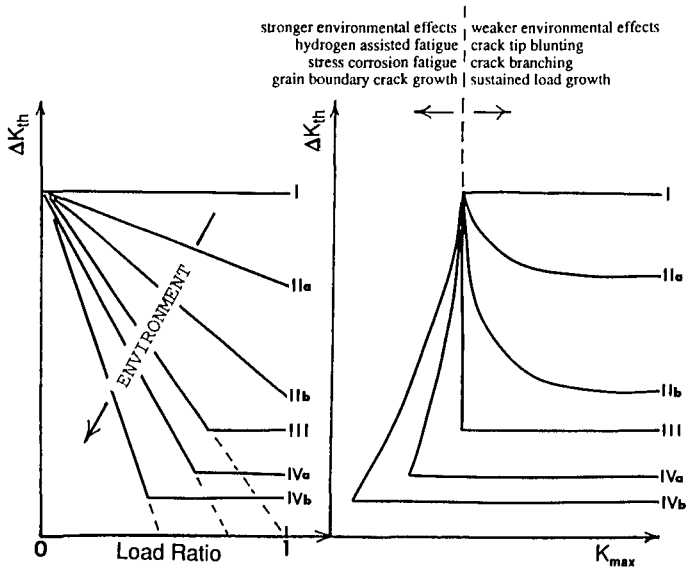


Figure 4. Schematic explanation of the overall fatigue mechanisms to indicate the four main classifications in terms of (a)  $\Delta K_{th}$  vs  $R$ , and (b)  $\Delta K_{th}$  vs  $K_{max}$ , along with the regions affected by the environment.

mechanism. In vacuum, the cyclic damage mechanism is mainly due to fatigue and is  $\Delta K_{th}$  controlled at all  $R > 0$ . With an increase in the aggressiveness of the environment,  $R^*$  would increase, implying that (a) range of  $R$  in which  $K_{max}$  was operating increases, and (b) the role of  $K_{max}^*$  increases at the expense of  $\Delta K_{th}^*$ . This increase role of  $K_{max}$  is related to the increased contribution from the crack-tip corrosion process in the environment.

### Classification of FCG

One can classify material behavior under fatigue loading into five different classes from the variations in  $\Delta K_{th}$  versus  $R$  at all  $R > 0$ . Here we restrict our discussion to the Classes I through IV. The materials under Class V is omitted, as they seem to fall under polymeric systems. Such classification methods help in recognizing the individual fatigue behavior of different family of materials and to understand the relative roles of the environment on fatigue. The basic concepts are applicable to fatigue from near-threshold region to all crack growth rates.

The basic scheme of classification is illustrated in Fig. 4a. Here Class II designated materials are labeled as a "normal" fatigue behavior, if the  $\Delta K_{th} - R$  curve extrapolation intersects the  $R$ -axis at  $R=1$  where  $\Delta K_{th} = 0$ . If the  $\Delta K_{th}$  intercept at  $R=1$  is greater than zero, we have termed it as Class II. In figure 4a, two different slopes are shown with Class II behavior to indicate that varieties of slopes are possible. In the limit, this Class II would converge to Class I where  $\Delta K_{th} - R$  slope approaches zero; while it can converge to Class III when the intercept approaches zero. Class IV (shown with two slopes) corresponds to the behavior when  $\Delta K_{th}$  intercept becomes less than zero at  $R=1$ . Experimentally the curve may level off prior to  $\Delta K_{th}$  reaches zero, as in Classes IVa and IVb, in figure 4a. Such a classification shows the role of the environmental effect giving rise to different slopes in  $\Delta K_{th}$  versus  $R$  curve; moving from Class I behavior (as in inert environment) to Class IV that corresponds to an aggressive environment.

Class II behavior is commonly observed in low strength / high ductility pure metals, in some medium strength alloys showing less environmental effects and in some high strength / high toughness alloys where crack-blunting process could be dominant. Class III type of behavior seems more common in al-base alloys in aqueous environment. Here  $\Delta K_{th}$  and  $K_{max}$  thresholds are uniquely defined. Class IV types are not common, but is observed in a few high strength materials that show strong environmental controlled fatigue, as in hydrogen-assisted fatigue of steels. Hence, the physics of crack-growth process in different classes of fatigue behavior is affected by the crack-tip environment. The experimental example for such a classification is shown in figure 5a, in terms of  $\Delta K_{th} - R$  plot and the corresponding  $\Delta K_{th} - K_{max}$  plot in figure 5b [6-11]. One can observe the similarity between the actual data in figure

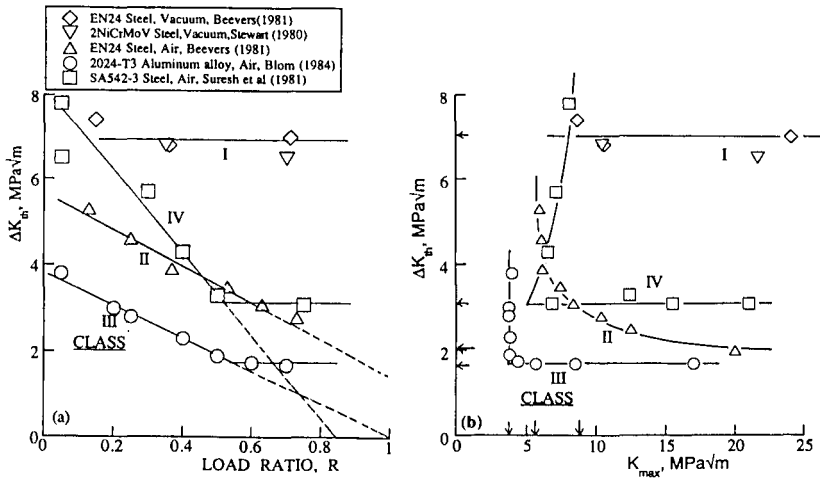


Figure 5. Experimental results showing the different class of fatigue behavior in terms of (a)  $\Delta K_{th}$  vs R, and (b)  $\Delta K_{th}$  vs  $K_{max}$ . The results were taken from aluminum and steel alloys.

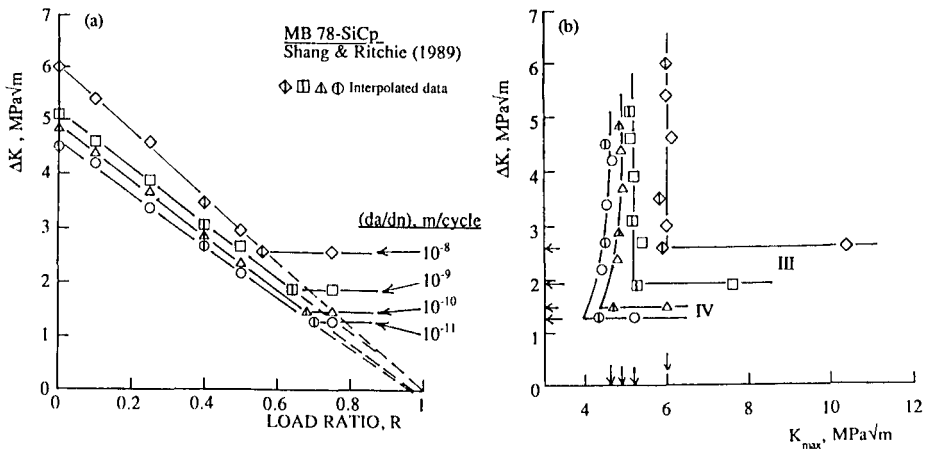


Figure 6. Class-IV MB-78-SiCp aluminum composites data extended to higher crack growth rates showing the transition from Class-IV to Class-III; in the form of (a)  $\Delta K_{th}$  vs R, and (b)  $\Delta K_{th}$  vs  $K_{max}$ .

5 to the hypothetical trends in figure 4. So far, we have discussed the FCG at near thresholds region. The classification scheme is also applicable to trends at higher crack growth rates.

As the fatigue behavior of the material changes with crack growth rates, the classification hierarchy moves towards lower classes. This is shown from the MB-78-SiCp aluminum composite [14], which starts with Class IV type behavior at near-threshold growth rates and transitions toward Class II at higher growth rates, figure 6. Unfortunately much higher growth rates data was not available to illustrate the transition to Class II and I behavior. As the crack growth rates increases from  $10^{-11}$  to  $10^{-8}$  m/cycle,  $K_{max}$  component becomes dominant, with the role of plasticity increasing with an attendant decrease in the role of environment. The relative mechanisms are listed schematically in Fig.4b.

### Summary

Fatigue crack growth (FCG) phenomena is intrinsically a two parametric problem, a concept that is independent of the existence of crack closure. The two loading parameters require two threshold driving forces that must be satisfied simultaneously for a crack to grow, and they both are strongly depend on the slip planarity and environment. The entire FCG behavior can be classified into five main classes, each pertaining to a given fatigue mechanism. The basic concepts suggest that for a complete fatigue it is necessary to get a systematic set of data at various load ratios and growth rates.

### References

1. R. A. Schmidt & P. C. Paris, ASTM STP-536 (1973) 79.
2. S. Suresh, Fatigue of Materials, (Cambridge University Press, 1991), Ch.7.
3. A. K. Vasudevan, K. Sadananda & N. Louat, Scripta Metall. et Materialia 27, (1993), 1673.
4. A. K. Vasudevan, K. Sadananda & N. Louat, Scripta Metall. et Materialia 28, (1993), 65.
5. A. K. Vasudevan, K. Sadananda & N. Louat, Scripta Metall. et Materialia 28, (1993), 837.
6. A. K. Vasudevan, K. Sadananda & N. Louat, Fatigue '93, ed. J.-P. Bailon and J. I. Dickson (EMAS Publ. UK, 1993), vol.I, 565.

7. A. K. Vasudevan, K. Sadananda & N. Louat, Fatigue '93, ed. J.-P. Baille and J. I. Dickson (EMAS Publ. UK, 1993), vol.I, 571.
8. K. Sadananda & A. K. Vasudevan, Aspects of High Temperature Deformation & Fracture in Crystalline Materials, ed. Y. Hosoi et al (JIM Publ. Japan, 1993), 551.
9. N. Louat, K. Sadananda, M. Duesbery & A. K. Vasudevan, Met. Trans. 24A, (1993), 2225.
10. K. Sadananda & A. K. Vasudevan, ASTM STP-1220, (1994), in press.
11. A. K. Vasudevan, K. Sadananda & N. Louat, Mater. Sci. Engg., (1994), a review, in press.
12. H. Kemper, B. Weiss & R. Stickler, Engg. Fract. Mech. 15A, (1989), 369.
13. A. K. Vasudevan & K. Sadananda, Mater. Trans. A, (1994), in press.
14. J. K. Shang & R. O. Ritchie, Met. Trans. 20A, (1989), 897.